Microbranching instability and the dynamic fracture of brittle materials

Eran Sharon and Jay Fineberg
The Racah Institute of Physics, The Hebrew University of Jerusalem, Givat Ram, Jerusalem, Israel
(Received 21 March 1996; revised manuscript received 31 May 1996)

We describe experiments on the dynamic fracture of the brittle plastic, PMMA. The results suggest a view of the fracture process that is based on the existence and subsequent evolution of an instability, which causes a single crack to become unstable to frustrated microscopic branching events. We demonstrate that a number of long-standing questions in the dynamic fracture of amorphous, brittle materials may be understood in this picture. Among these are the transition to crack branching, ''roughness'' and the origin of nontrivial fracture surface, oscillations in the velocity of a moving crack, the origin of the large increase in the energy dissipation of a crack with its velocity, and the large discrepancy between the theoretically predicted asymptotic velocity of a crack and its observed maximal value. Also presented are data describing both microbranch distribution and evidence of a new three-dimensional to two-dimensional transition as the ''correlation width'' of a microbranch diverges at high propagation velocities. [S0163-1829(96)05034-5]

I. INTRODUCTION

For many years, a great deal of both theoretical and experimental work has been dedicated to understanding the phenomenon of dynamic fracture. When, in the presence of a crack, an elastic medium is subject to externally applied stress, the energy stored in the elastic field is focused into the crack's tip. Above a threshold value of applied stress, the crack will propagate, thereby creating new surface. If the fracture energy (defined as the amount of energy needed to create a unit surface) is known, the characteristics of the stress field around the crack tip, as well as the equation of motion of a single crack can be derived.[1] These calculations, which assume that the medium behaves according to the equations of linear elasticity and that the crack propagates along a straight line, predict that a crack should smoothly accelerate to the limiting value of the Rayleigh wave speed, V_R, of the material.

Models of a *single* crack, however, have had difficulties in predicting experimental results. Experimentally, the limiting velocity of a crack reaches about half of the predicted value[2] and the observed increase of the fracture energy, γ, with the crack velocity, v, lacks a quantitative explanation. Another long-standing problem is the mechanism for the formation of nontrivial fracture surface. Whereas the analytic treatment assumes that a crack will travel in a straight-line trajectory, the fracture surface formed by a crack becomes increasingly rough as the crack velocity increases.

An alternative view, that the fracture process is due to the coalescence of microvoids or preexisting defects situated in the crack's path, has been proposed.[3] In this picture, defects ahead of the crack will start to propagate due to the intense stress field at the crack tip. This idea was supported by a series of experiments by Ravi-Chandar and Knauss[4] on the brittle plastic, Homolite 100, where the simultaneous propagation of an ensemble of microcracks, instead of a single propagating crack, was observed. Increased energy flux to the tip, in this view, would increase the number of microcracks formed thereby creating a mechanism for enhanced dissipation. As defects exist in most materials, the above picture would suggest that crack propagation via interacting microvoids should, in general, occur as a randomly activated process. Although this picture is appealing, a theoretical description relating the dynamics of a crack ensemble to both the flux of energy into the crack and microcrack production has not been forthcoming.

An additional problem in dynamic fracture is that of crack branching, where, when sufficiently high stress is applied, a single crack will bifurcate to a state of two propagating cracks. Although a number of criteria for crack branching have been suggested,[5] none of these agree with experiment. A criterion based on the dynamics of a crack was first suggested by Yoffe[6] with similar criteria following.[1] The Yoffe criterion follows from a calculation of the *singular component* of the stress field at the tip of a crack moving at constant velocity. Yoffe found that the singular component of the stress field normal to any given direction is maximal in the X (or propagation) direction until a critical velocity $0.6c_T$, where c_T is the transverse wave speed of the material. Above this velocity, the normal stress component is maximal at an angle which continually increases with v, reaching about 60° relative to the propagation (X) direction. This condition implies that a single straight crack at this velocity should become unstable and result in crack branching. Experiments, however, indicate that large-scale crack branching occurs at velocities far below the critical velocity predicted by Yoffe[7] (although a recent theory by Gao[8] predicts that due to nonlinearity, the *local* Rayleigh wave speed at the tip of the crack may be much lower than linear elasticity would predict) with measured branching angles[9] between 10° and 15° in a variety of brittle materials. In addition, recent calculations[10] suggest that a single propagating crack may *always* be unstable to a Yoffe-like instability. The observed branching angles agree with predictions of the branching angle resulting from the ''far-field'' stress field of a moving crack.[11] Although the Yoffe criterion predicts a critical velocity for crack branching which is independent of boundary conditions, experiments also show that crack branching occurs at different velocities and depends on the loading conditions.[12]

Experimental observation of crack branching events all describe macroscopic branches, or ''successful branching events,'' which are affected by the stress field far from the tip of the main crack. Hence, the singular term of the stress field, on its own, cannot properly describe the problem and measurements of such events should not be expected to obey the Yoffe criterion. In what follows, we will describe observations of microbranches or frustrated branching events occurring at scales where the singular stress field in the vicinity of the crack tip should be the dominant component of the stress field. In this case, we may expect such criteria to be relevant and we may see behavior reminiscent of Yoffe's predictions. As we will show, in this near-tip region the behavior of a microbranch is indeed qualitatively different than that of macroscopic crack branches.

In this paper we review a series of recent experiments performed on PMMA (poly-methyl-methacrylate). The results of these experiments offer a new view of the fracture process. We will show that the transition from a single-crack to a multicrack state is the result of a *dynamic instability.* This instability appears as the velocity of the crack exceeds a critical velocity, $v_c = 0.36V_R$. Below v_c a single crack is observed, the crack velocity is a smooth function of time (increasing or constant, depending on experimental conditions) and the fracture surface created is smooth and mirrorlike. Beyond v_c, a single-crack state no longer exists. Instead, a crack will sprout small microscopic side branches (microbranches) whose dynamics are interrelated with those of the main crack. As a function of the mean velocity, v, these branches increase in length as the mean dynamics of a crack change dramatically; the crack velocity develops oscillations, and nontrivial structure is formed on the fracture surface.[13,14] Both the oscillations in the crack velocity and the amplitude of the structure formed on the fracture surface scale with the length of the microbranches. As the branches grow in size, they evolve into macroscopic, large-scale crack branches. Thus, the instability is actually the conduit that provides the crucial link between a single-crack state, at low-energy flux (low velocities) and the multicrack states, which include both microcrack states and macroscopic branching, at high-energy fluxes. The general nature of this instability is suggested by the acoustic emissions[15] of moving cracks in both PMMA and glass, where large-amplitude emission centered at well-defined frequencies appear in both materials as the crack velocity surpasses $0.4V_R$.

By quantitative measurement of both the energy flux into the tip of a moving crack and the total amount of surface area created in PMMA, we will also show that the microbranching instability is the main mechanism for the increase in the dissipation of energy by a moving crack at high velocities.[16] We will demonstrate that the rate of new surface creation, beyond v_c, is proportional to the energy flux into the tip of the crack. This mechanism provides a simple explanation for both the observed velocity dependence of the fracture energy and for the question of why the limiting velocity of a crack, the Rayleigh wave speed, is never realized.

The above experimental observations support recent theoretical work. Marder and Liu[17] modeled brittle elastic media as a two-dimensional (2D) lattice of coupled springs with a small rate-dependent dissipative term. The springs, in this model, are perfectly elastic up to a critical displacement at which point they snap. The system is driven, as in our experiments, by constant displacement of the system's boundaries in the direction normal to propagation. The model reproduces the Yoffe instability; a single straight crack moving in a homogeneously stressed infinite strip is no longer a stable solution at velocities above $0.6V_R$. Numerical solution of the model for $v > 0.6V_R$ exhibit the periodic occurrence of local branching events where the main crack sprouts side branches that propagate for a short distance and die. In finite element calculations performed by Johnson[18] and Needleman[19] models for plastic deformation of the material in the near vicinity (called the process zone) of the crack tip are included. In both calculations the crack is driven by an abrupt increase of the load behind the crack, steady-state propagation is not reached, and frustrated branching events at velocities lower than $0.6V_R$ were observed. Johnson observed a sharp increase in the energy released by the crack at every branching event. The branching events observed by Needleman precipitated a sharp decrease in the velocity of the main crack, which then reaccelerated after the branch's ''death.'' In this model, an initial branching angle of 29° to the propagation direction (X direction) was observed and, as they developed, the branches tended to align parallel to the main crack. The same tendency of a decreasing angle of branch propagation was observed by Parletun[20] in simulations based on the static stress field at the crack tip in the early stages of crack branching, and Isida *et al.*[21] using a perturbative calculation of static stress fields for finite-sized cracks. Our analysis of the Parletun data indicate that the branch profile, in its early stages of propagation, obeys a power-law relation of approximately $y \propto x^{0.78}$ where the Y direction is defined as that parallel to the direction of applied stress. Isida *et al.* predict an initial branching angle of 27.3° which rapidly decreases with the length of the branch.

Dynamic instability of crack growth was also observed in recent molecular simulations of a 2D triangular lattice using a Lennard-Jones potential.[22] In these simulations, velocity oscillations, attempted crack branching, and an increase in surface roughness, appear once the crack velocity exceeds a critical velocity of $0.32V_R$. The good quantitative agreement between these simulations and experiment as well as the qualitative agreement with experiment observed in the different models described above, lends credence to the general character of both the instability and the resulting behavior of the crack that will be detailed below.

II. EXPERIMENTAL SYSTEM

Before reviewing our results we will first briefly describe the experimental system, presented schematically in Fig. 1. A more detailed description can be found in Ref. 13. The experiments were conducted in thin, quasi-2D sheets of brittle, cast PMMA,[23] having a thickness (Z direction) of either 0.8 mm or 3 mm with vertical (Y direction) and horizontal (X direction) dimension between 50 and 200 and 200 and 400 mm, respectively. Stress was applied to the sample via steel bars, which were straight to within 10 μm tolerances, and glued to the opposing faces of the sample at each of its vertical boundaries. All samples were loaded via uniform displacement of the vertical boundaries with the fracture initiated at constant displacement. Applied stresses in

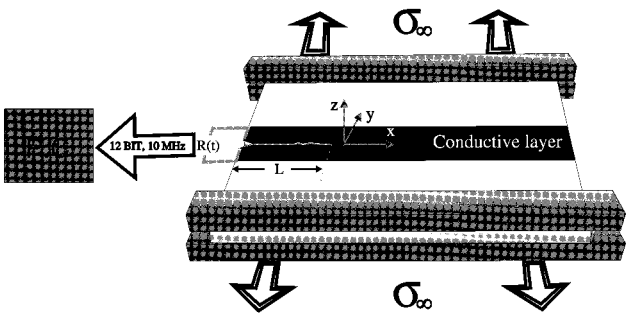

FIG. 1. A schematic view of the experimental system. Steel bars are glued to opposite surfaces of a rectangular PMMA sheet with an initial seed crack in its center. The stress, σ_∞ ,is applied via uniform quasistatic displacement of the bars. THE center of the plate is coated with a 30-mm-wide strip of a thin (1-μm-thick) conductive layer. As the crack propagates across the sample, it cuts the conductive layer and changes its resistance. The instantaneous resistance of the conductive layer is found by measuring the voltage drop across it at 10-MHz rate to 12-bit resolution. A straight crack, of length L, running through the center of the strip, will produce a ''strip resistor'' of length $2L$ and width 15 mm, leading to nearly linear relation between the location of the crack tip and the resistance of the plate.

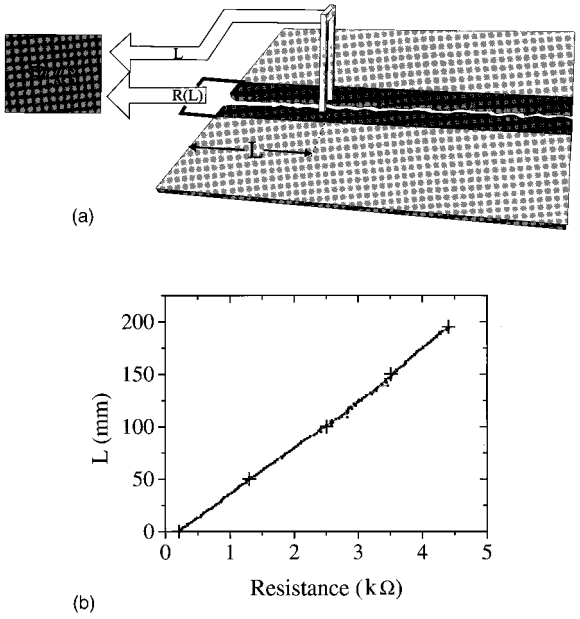

FIG. 2. (a) Resistance calibration system. An electric contact connecting opposing points of the conductive layer which were separated by the crack, is pulled quasistatically along the crack's path. The resistance, R of the conducive strip is thus measured as a function of the location of the electric contact (L). Inhomogeneities in the conductive layer, as well as deviations of the crack from a straight line, will cause a nonlinear $R(L)$ profile. This profile is used to calibrate the dynamic fracture measurement (se Fig. 1). (b) A typical calibration measurement. The resistance measurements (squares) are fitted by a fifth-order polynomial (solid line). The crosses shown are calibration points obtained by the use of discrete conductive strips, located on the opposite face of the plate, and cut by the crack as it progresses across the plate.

the experiments were varied between 10 and 18 MPa. Prior to loading, a small ''seed'' crack was introduced at the edge of the sample midway between the vertical boundaries. Tensile stress (mode I loading) was then applied quasistatically until arriving at the desired stress. Crack propagation was then initiated by gentle application of a razor blade in order to sharpen the initial crack.

The sample geometry was varied to provide either steady-state crack propagation at a constant energy density within the sample, or a continuously changing velocity throughout the experiment. Steady-state propagation was achieved by using the thin-strip configuration with the ratio of its vertical to horizontal dimensions between 0.25 and 0.5. When the crack tip is sufficiently far from the horizontal boundaries of the system, this geometry approximates an infinitely long strip with approximate ''translational invariance'' in the direction of propagation. This state is realized when the crack reaches a length of about half of the vertical size of the system. At this point, advance of the crack by a unit length frees an amount of energy equal to the (constant) energy per unit length stored in the plate far ahead of the crack. Under these conditions, a crack arrives at a state of constant mean velocity with G, the energy flux into the crack tip power unit extension of the crack, given by $G=\sigma^2 L/(2E)$. Here σ is the applied stress at the vertical boundaries, L the vertical size of the system, and E Young's modulus of the material. The value of $E=2.8\times10^9$ N/m^2 used for PMMA was obtained by quasistatic measurement of a plate of the dimensions and manufacture used in the experiments. With this geometry we can directly measure G with an 8% accuracy. In the experiments described, G was varied between 400 and 5000 J/m$_2$.

The crack velocity was measured by first coating the side(s) of the sample with a thin (0.1–1 μm) resistive layer. Upon fracture initiation, a propagating crack will cut the resistive coating thereby changing the sample's resistance. The coated area was 30 mm wide (in the Y direction), and the electric leads were connected to either side of the seed crack. With this geometry we obtain a nearly linear relation between the crack length and the resistance of the coated plate, as shown in Fig. 1. As the crack propagates across the sample, we measure its resistance change by digitizing to 12-bit accuracy at a rate of 10 MHz. Thus, in PMMA, the location of the crack tip can be established with a 0.1 mm spatial resolution at 0.1 μs interval yielding a velocity resolution of better than 25 m/s. The linear relation between the crack length and sample resistance can be perturbed by either resistance variations due to any inhomogeneity of the resistive layer and/or any overall deviation of the crack's path from the midplane of the layer. To correct for these variations, we calibrate the sample resistance after each experiment as shown in Fig. 2(a). This is done by measuring the sample resistance, as a function of the location of a soft metal ball contact, which is pulled along the path of the crack so that it electrically reconnects both faces of the sample at the point at which they were separated by the crack. We then fit the data to a fifth-order polynomial, as shown in Fig. 2(b), which is then used to obtain the final relation between the crack length and plate resistance.

After fracture, the crack profile in the XY plane was measured optically with a spatial resolution of 1–5 μm, depending on the magnification used. Although the medium is ide-

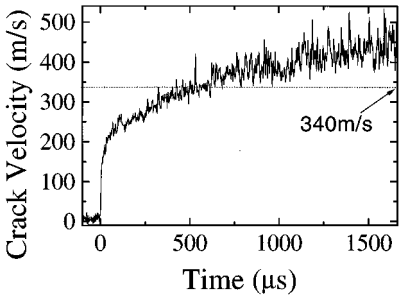

FIG. 3. A typical measurement of the velocity of a crack tip as a function of time. After an initial jump to about 150 m/s, the crack accelerates smoothly up to the critical velocity of $v_c = 10$m/s. Above v_c strong oscillations in the velocity of the crack are observed.

alized as 2D, the plates used are of finite thickness. All comparisons between the crack's profile and velocity were made using measurements taken adjacent to the plane where the velocity measurements were performed. Additional measurements of the fracture surface profiles and surface roughness were performed by means of an X-Z scanning profilometer with a resolution of 0.1 μm in the Y direction. Both the optical and profilometer measurements were correlated with the velocity measurements.

III RESULTS

The instability is apparent in the three different types of diagnostics performed: velocity measurements, measurements of the fracture surface, and the optical measurements taken in the X-Y plane. As we shall see, these three aspects of the instability are interrelated. We can follow their development as either a function of the mean velocity or of the energy flux to the crack tip, G. In Fig. 3 we present a typical velocity measurement of a crack in a PMMA plate. After a nearly instantaneous jump to an initial velocity (typically between 0.1 and $0.2V_R$) the crack accelerates smoothly until reaching the critical velocity, $v_C = 340$m/s (or $0.36V_R$). As the crack velocity exceeds v_c, it develops strong oscillations, which increase in amplitude with the mean velocity of the crack.

A series of velocity measurements at $v < v_c$, $v \sim v_c$, and $v > v_c$ are presented in Fig. 4(a). Examining the fracture surface formed at these velocities [Fig. 4(b)], one finds that as long as the crack velocity is below v_c, the fracture surface is ''mirrors'' like with no apparent features at scales larger than 1 μm. As the crack velocity reaches the critical velocity, small localized features appear on the fracture surface. At higher velocities these surface feature coalesce and evolve into a periodic riblike pattern with the spacing between ribs on the order of 1 mm. On this scale PMMA is entirely amorphous.

Scanning the fracture surface in the X-Y plane [Fig. 4(c)], one finds that below v_c fracture is described by a single crack. At $v \sim v_c$ small side branches appear. These grow larger as the mean velocity of the crack increases. In Ref. 13 the instability threshold of $v_c = 340$ m/s for the onset of both velocity oscillations and the appearance of surface structure was shown to be independent of the sample thickness, lateral dimensions of the plate, the surrounding atmosphere, and the external loading. In Fig. 5 we demonstrate that the same threshold exists for the onset of microbranching. As the sample loading is increased, the acceleration and the maximal velocity may increase but the appearance of both structure on the fracture surface and microbranches will always occur at the same threshold of $v_c = 340 \pm 10$ m/s.

A. Characterization of the branching instability

Looking at pictures of the fracture surface when the instability is well developed [see Fig. 4(b)], we note the characteristic pattern that is created on the fracture surface. Careful examination of the spacing between the ribs on the fracture surface indicates that the ''wavelength'' of the patterns is not constant but is instead a linear function of the mean velocity. As observed in Ref. 13, the instability has a well-defined *time* scale as shown in Fig. 6 where we present a power spectrum of the crack velocity fluctuations. Although the

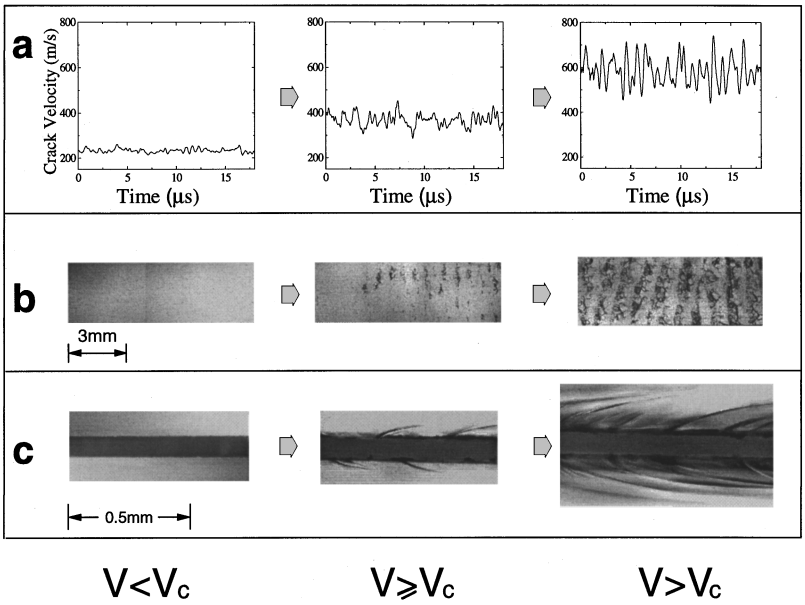

FIG. 4. Three aspects of the evolution of the branching instability as the crack propagates from left to right. (a) The velocity of the crack is a smooth function of time for $v = 300$ m/s $< v_c$ (left), at $v = 400$ m/s $\sim v_c$ the crack velocity starts to oscillate (center), the oscillation amplitudes increase at higher velocity (right). (b) For $v = 300$ m/s $< v_c$ the fracture surface is smooth (left), at $v \sim 400$ m/s small regions of different texture are distributed along the surface (center). At $v \sim 400$ m/s small regions of different texture are distributed along the surface (center). At $v \sim 600$ m/s these regions coalesce, forming a periodic pattern with wavelength on the order of 1 mm (right). (c) A single crack is observed (left) for $v < v_c$. Microbranches appear at $v \cong v_c$ (center), and increase in length at higher velocities (right).

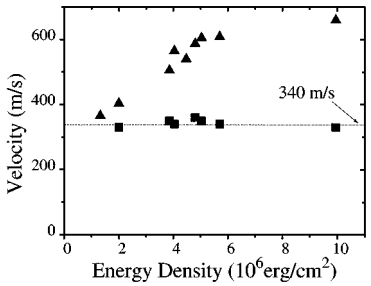

FIG. 5. The critical velocity for the observation of microbranching (squares) compared to the final steady-state crack velocities (triangles), as a function of the energy density stored in the material. While the steady-state velocity depends on the external loading, the microbranching velocity is independent of the driving. The energy density was obtained using samples in the strip configuration. The critical microbranching velocity is the average (over 1 cm) of the crack velocity at the locatio where the first microbranches are observed.

spectrum does not show a single sharp frequency, a well-defined time scale of 1–2 μs is apparent. Below v_c this scale is not observed, but for $v > v_c$ this characteristic time scale appears and is independent of the mean velocity of the crack as well as the lateral dimensions or thickness of the material.

The mean spacing between microbranches shows the same behavior, as seen in Fig. 7. The average distance between sequential microbranches increases linearly with the mean velocity so that, as the velocity of the crack increases, there are *fewer* branching events. Thus, as for the case of the velocity fluctuations, the mean *time* between the formation of sequential branches is constant with a value of 0.26 μs.

A further look at the microbranch spacing shows, as can be seen in Fig. 4(c), that the spacing between consecutive microbranches is broadly distributed. A typical probability distribution of the distances between neighboring branches is presented in Fig. 8 for a crack moving at a constant (steady-state) crack velocity. The data support a log-normal distribution. The same log-normal-type distribution is observed in the probability distribution of branch lengths presented in Fig. 9. It has long been known that the distribution of the fragment size of crushed or fractured objects[24] is log normal. The explanation for this is based on a picture dating back to Kolmogoroff[25] where a cascade of repeated fragmentation was assumed. For this explanation to be relevant, each individual fragment must be able to break with a constant probability. The data presented in Figs. 8 and 9 suggest a qualitatively different explanation for this distribution. These data indicate that the observed log-normal distribution can arise dynamically, as a result of a single fracture event, and not necessarily as a result of repeated fracture events. An important feature to note in the branch length distribution (inset of Fig. 9) is the existence of a nonzero *minimum* branch length. The minimum branch length of approximately 30 μm is independent of the mean velocity of the crack. The branch length distribution is characterized by its mean, $\langle L \rangle$, and width, σ_{br}, which are both completely defined by the mean crack velocity. The (identical) linear dependence of both parameters on the velocity, as shown in Fig. 10 indicates that the entire branch length distribution scales linearly with the crack velocity. Similar scaling occurs for the distributions of the distance between branches, as indicated in Fig. 7.

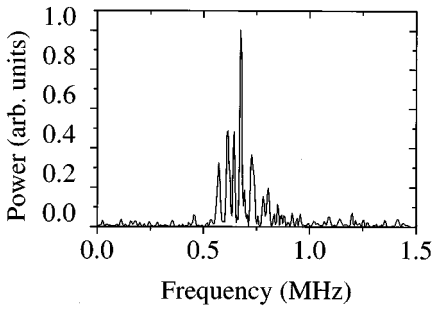

FIG. 6. A typical power spectrum of the crack velocity fluctuations at a steady-state velocity of 500 m/s. The maximum of the spectrum, at 600 KHz, is not dependent on the mean velocity.

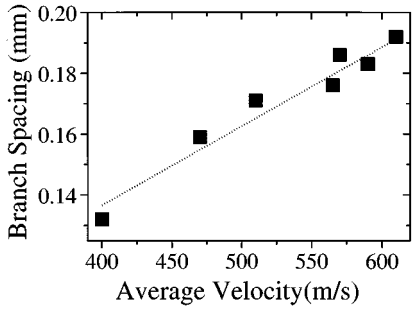

FIG. 7. The mean spacing between microbranches as a function of the mean velocity of the crack. The data points shown are the average values of over 600 branches at each steady-state velocity. The linear dependence indicates that, on average, microbranches are formed at a constant rate. The mean time of 0.26 μs between consecutive branches is determined by a linear fit of the data (dotted line).

We have seen that the dynamic instability that occurs beyond v_c can be identified by either the onset of velocity fluctuations of increasing amplitude, the appearance of struc-

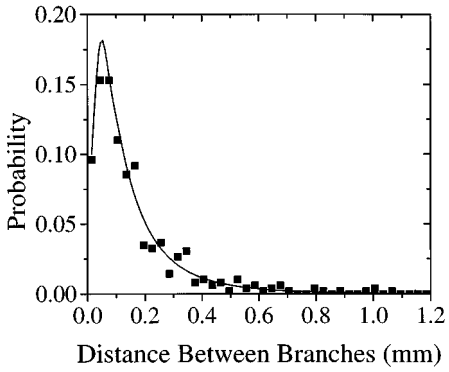

FIG. 8. A typical probability distribution of the distance between consecutive branches (squares) indicates a log-normal dependence (solid line). The data include 700 branches produced at steady-state velocity of 600 m/s. The data were binned with 0.03-mm interval. At different velocities the distributions are shifted in accordance with the mean velocity but they preserve their log-normal appearance.

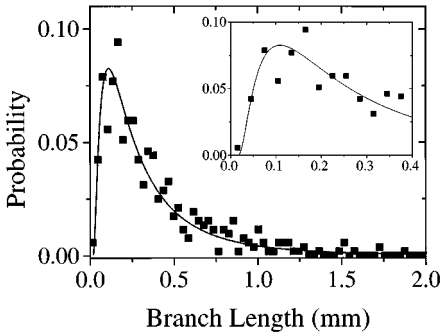

FIG. 9. A typical probability distribution of the length of microbranches (squares). The data include 700 branches, produced at steady-state velocity of 585 m/s. As in Fig. 8, the data are well described by a log-normal distribution (solid line). To obtain the plot, the data were binned in 0.03-mm intervals. Inset: The initial section of the distribution shown on an expanded scale. Note the existence of a minimum branch length of ~30 μm. This same minimum branch length value is also observed at other velocities. At different velocities the distributions are shifted in accordance with the mean velocity but they preserve their log-normal form.

ture on the fracture surface, or the initiation of microbranches. We now look at the characterization of these three different aspects of the instability as the instability develops. It is convenient to treat the mean velocity of the crack as a control parameter and describe the evolution of the instability as v increases. In Fig. 11 we compare the mean branch length, the rms amplitude of the fracture surface features (for a detailed description of these measurements see Ref. 13), and the rms amplitude of the fluctuations in the crack velocity, as a function of the mean crack velocity. As the figure shows, there is a well-defined functional dependence between these quantities and v which is independent of both the sample geometry and loading conditions.

The sharp transition between a single crack and a state with microbranches always occurs at the same critical velocity. After a jump to its minimum value (noted earlier in Fig. 9) the mean branch length [Fig. 11(a)] increases linearly as a function of the mean velocity, from v_c until at least 600 m/s. (Due to limitations of the measuring technique, we could not reliably measure all of the branches created at velocities

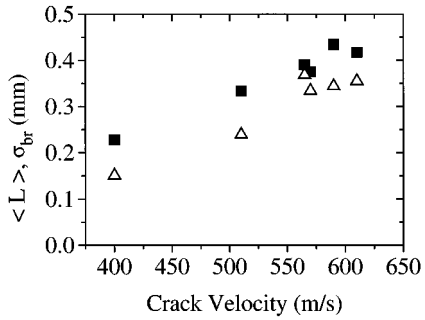

FIG. 10. The mean, $\langle L \rangle$ (squares), and standard deviation, $\sigma_{\rm br}$ (triangles), of the branch length distribution as a function of the crack velocity. Both increase linearly with the crack velocity and have the same slope. Thus, the entire distribution scales linearly with the velocity.

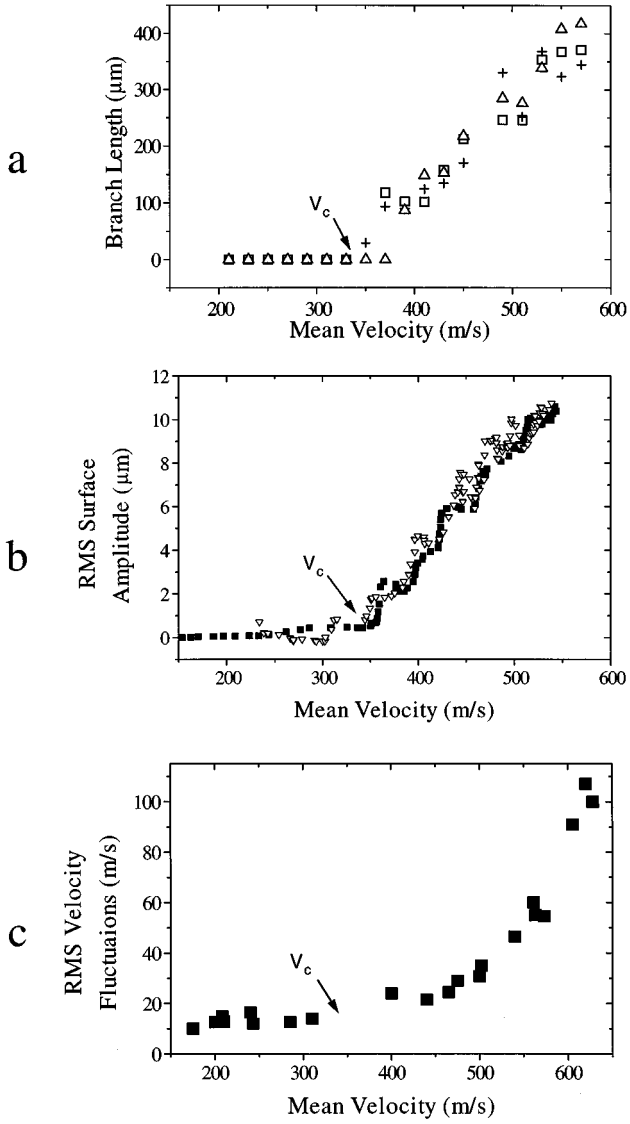

FIG. 11. The mean branch length (a), the rms value of the fracture surface amplitude (b), and the rms velocity fluctuations (c), as a function of the mean velocity of the crack. The arrows indicate the critical velocity of 340 m/s. The data in (a) and (b) were collected using accelerating cracks in plates of different geometries and different loading stresses. Note the nearly 2-order-or-magnitude difference in scales between the mean branch length and fracture surface amplitude data. The velocity fluctuations were measured at steady-state velocities. Although velocity fluctuations are indicated for $v < v_c$, a sharp rise in their amplitude occurs above v_c.

higher than 600 m/s but a qualitative increase in the mean branch length with increased mean velocity is observed.) The slope of this curve yields a characteristic time scale of 1 μs as the typical lifetime of a microbranch of any length in this range of velocities.

In both Figs. 11(a) and 11(b) we observe a sharp transition at v_c from a state of smooth surface to a state where the quantity measured increases linearly with the mean velocity of the crack. Note that although the two figures appear markedly similar, a comparison of the scales in both graphs reveals that the mean branch length is nearly 2 order of magnitude larger than the surface amplitude. This implies that

the structure on the fracture surface may well be formed as a *result* of the microbranching process. As can be seen in Fig. 11(c), although measurable fluctuations of the velocity exist before the instability onset, a sharp rise in the velocity fluctuations at $v > v_c$ is apparent. The velocity fluctuations can also be understood to result from the microbranching. As demonstrated in Ref. 14 the instantaneous crack velocity is correlated with the amount of surface created by microbranches at the same point and supports the following picture.[14,26] As a crack accelerates, the energy released from the potential energy stored in the plate is channeled into creating new surface (the two crack faces). When the crack velocity reaches v_c, the energy flowing into the tip of the crack is now divided between the main crack and the ''daughter'' cracks which are formed by branching events. Thus, unless energy is directed into each crack and the crack front velocity decreases. The daughter cracks, competing with the main crack, have a finite lifetime [of about 1 μs as indicated in Fig. 11(a)], presumably because the main crack can ''outrun'' and screen them from the surrounding stress field. The daughter cracks then die and the energy that had been diverted from the main crack returns causing it to accelerate until, once again, the scenario repeats itself. This mechanism of deceleration and acceleration was also observed in the finite element simulations in Ref. 19.

B. Pattern formation by a crack

We now examine the shape and structure of both the microbranches and fracture surface. Let us first turn to the functional form of the microbranches. As we saw in Fig. 4(b), at a given crack velocity the observed lengths of the microbranches are broadly distributed. In Ref. 14 it was shown that the functional form of these branches is not random but surprisingly well-defined. Although the lengths of microbranches have a wide distribution, a branch, once formed, follows a distinct trajectory of the form (for $v = 1.09 v_c$) $y = 0.2 x^{0.70}$, where y is the normal and x the direction parallel to the propagation direction of the main crack. For crack velocities within 10% of $v_c$the scatter in the microbranch profile is relatively small. (The scatter is on the order of the ± 3 μm uncertainty in the starting point of a given branch.) As shown in Fig. 12, at higher velocities the mean profile of the branches exhibits the same exponent, while the coefficients increase slightly. In addition, the scatter in the branch profiles increases with v, becoming several times the measurement uncertainty at velocities 40% over v_c.

We now turn to the question of the branching ''angle.'' If the observed power-law profile of a branch holds down to microscopic scales, we should see a continuous increase of the apparent branching angle with each decrease in the scale of observation. At scales of 0.1–0.3 mm (the scales at which macroscopic branching phenomena are typically measured) the ''branching angle'' given by the power-law profile is between 10° and 15°, as commonly reported in the literature. At the smallest spatial scales measured (between 3 and 5 μm, set by the diffraction limit of our optics), we find the branching angle to be normally distributed around 31° as Fig. 13 indicates. This result is independent of the crack velocity. At these scales, the value of the branching angle measured agrees well with the 27.3° observed in Ref. 21, the

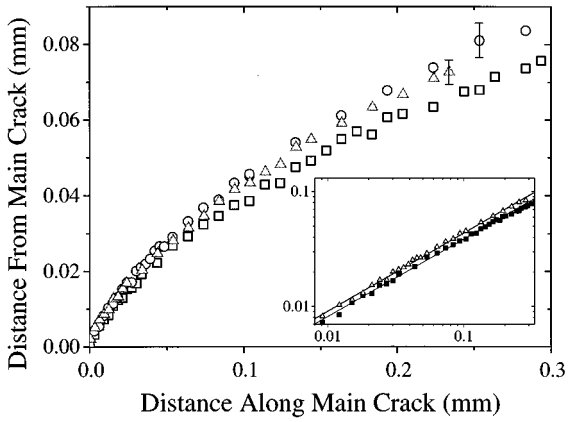

FIG. 12. The mean profile of microbranches obtained for differnt propagation velocities: 374 m/s (squares), 407 m/s (triangles) and 470 m/s (circles). As the velocity increases, the 0.7 exponent remains, while the coefficient of the mean profile increases (0.18 at 374 m/s, 0.2 at 470 m/s). This is demonstrated in the inset for $v = 374$ m/s (squares) and 470 m/s (triangles) on a log-log scale. In addition, the scatter, as indicated by the error bars, increases with the mean propagation velocity.

29° observed in the finite element simulations[19] and the 30° branching angle seen in the molecular dynamical simulations[22] but we cannot rule out either the 60° angle predicted by Yoffe or the 90° branching angle that would true of a power-law branch profile at the smallest scales. These large branching angles at microscopic scales are due to the influence of the singular term of the stress field in the near vicinity of the crack tip. As the microbranches grow and increase their separation from the main crack, the influence of the higher-order terms of the stress field increases. Thus, there is no conflict between our observations and the predictions corresponding to the small (macroscopic) branching angles, which were based on the ''far-field'' values of the stress field far from the crack tip.

How does the morphology of the fracture surface relate to the microbranches? Figure 14 shows a closeup of the fracture surface, which includes the periodic patterns observed at

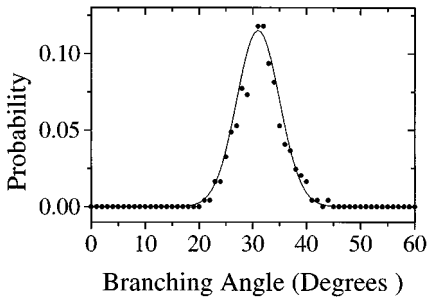

FIG. 13. A probability distribution of the branching angle of microbranches. The data include 250 branches, produced at velocities between 400 and 600 m/s. The spatial resolution of the measurement was 3 μm. The branching angle is defined as the angle between the main crack and the line connecting the branching point with a point on the microbranch located 3–5 μm from the branching point.

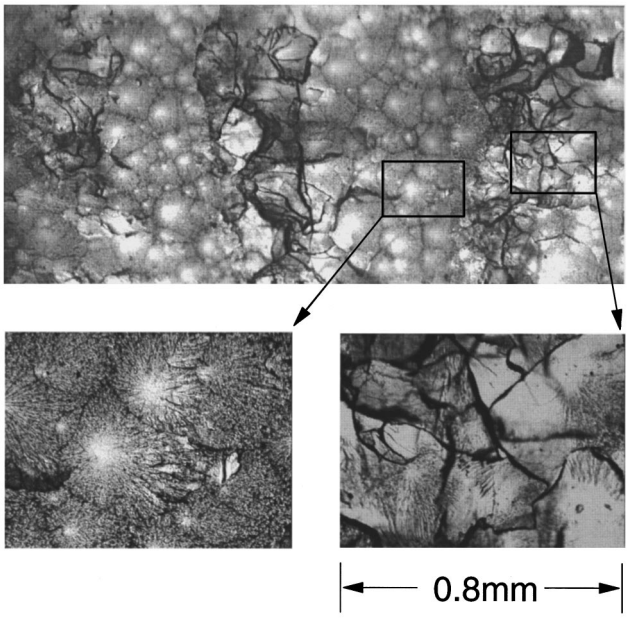

FIG. 14. A photograph of the typical surface formed by a crack moving from left to right at 600 m/s. The pattern observed on the fracture surface has the appearance of periodic ''cleavage'' events. Unlike the rest of the fracture surface, which has a ductile nature, indicated by the parabolic marks and the rippling structures (bottom left), the strips (bottom right) appear to be composed of separate plates having a ''glassy'' surface reminiscent of cleavage planes.

high velocities. As we see in the figure, the patterns are not simple undulations of the fracture surface, but there is a clear morphological difference between them and the rest of the surface. The surface between patterns (like the fracture surface prior to the instability) is reminiscent of ductile fracture with the well-known parabolic and ripple marks evident. The surfaces producing the observed periodic patterns are different; instead of the ripple marks we find that the surface appears to be broken into separate facets composed of smooth, glasslike material. It is possible that these patterns occur at either high crack separation rates or (more on this later) within the process zone of the main crack where the material becomes more ''brittle'' and apt to ''cleave.'' In both cases the material cannot flow and the surrounding material is not deformed by the microbranch.

The structure observed on the fracture surface is formed by the initial part of a microbranch while the remainder of the microbranch continues inside the material. Figure 15 presents views of a section of the fracture surface from both the top (XZ plane) and side (XY plane). From the figure it is clear that the microbranches appear beneath the patterns on the fracture surface. Above the large branches in the XY plane there are noticeable upheavals of the fracture surface corresponding to the facets viewed in the XZ plane. These surface upheavals mark the onset of microbranches that penetrate the opposing crack surface. This close connection between the surface roughness and microbranch size explains the strong similarity of Figs. 11(a) and 11(b). If, as we suggest, the features on the fracture surface are indeed the initial stages of the microbranches, the *form* of the surface features should follow the branch profiles. Thus, we expect the amplitude of the surface features to scale as the 0.7 power of their length like the branch profiles presented in Fig. 12. This may provide an explanation for the scaling behavior of a fracture surface that has been observed in many materials.[27] The roughness of a fracture surface, σ, is defined as the rms deviation of the surface height from its mean value. A number of recent experiments have observed that $\sigma \sim L\zeta$ where L is the measurement scale in the direction of propagation. The measured value of 0.7 for the ''roughness exponent,'' ζ, has been conjectured to be universal in brittle two-dimensional materials.[28] Using the scaling relation $y \propto x^{0.7}$ for the functional form of a branch we obtain a roughness exponent of 0.7 for sizes smaller than the typical spatial extent of a local branch. This explanation of surface roughness would suggest that the region where σ is observed to exhibit scaling behavior may be limited to these sizes and is thereby a function of the mean velocity of a crack or alternatively the energy dissipated by the system.

C. Energy dissipation by a crack

As mentioned in the Introduction, one of the outstanding problems in dynamic fracture is the fact that the predicted limiting velocity for a crack, the Rayleigh wave speed, is never reached. Normally a crack reaches just about half of V_R. One explanation for this is an apparent sharp increase in the fracture energy with increasing crack velocity. In PMMA, the increase in the energy release rate, G, defined as the energy flux to the crack tip per unit crack extension, is as

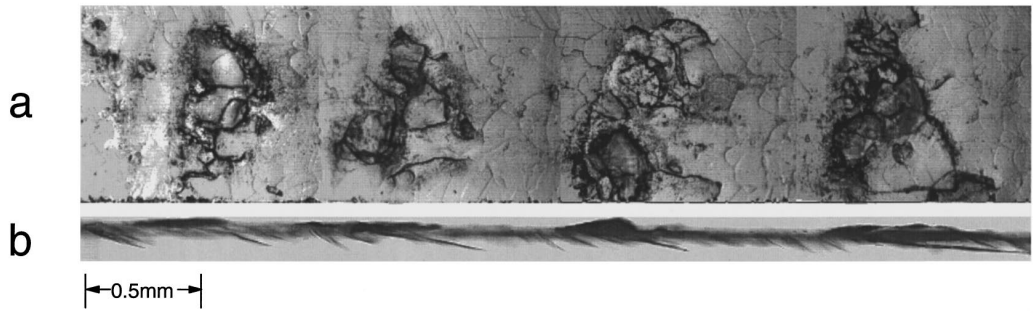

FIG. 15. (a) A top (XZ plane) view and (b) a side (XY plane) view of a section of the surface formed by a crack moving with velocity of 600 m/s in a 0.8-mm-thick plate. Note the appearance of large branches beneath the ''cleavage zones'' on the fracture surface. We view the large ''upheavals,'' situated above the large microbranches on the fracture surface, as marking the onset of microbranches that penetrate the opposing crack surface.

much as an order of magnitude[16,29] as v increases between 300 and 600 m/s. Previous work has shown that the majority of the energy flowing into the crack tip ends up as heat[30] with a maximum of about 3% of G radiated away from the near vicinity of the crack as acoustic emissions.[15] No general mechanics, however, has been suggested for purely brittle materials which can explain this extensive increase in dissipation as the crack velocity increases. Considering the internal structure of PMMA, which consists of very long tangled molecules, one might expect that the energy cost for the creation of a unit fracture surface, would be determined by complex, rate-dependent mechanisms which include both plastic deformation of the material together with the heat production involved in craze formation.[31] Yet, since PMMA is a brittle material, the dissipation associated with the flow of the material before fracture must be limited.

How does the large increase in fracture energy as a function of v occur? The ''microbranching'' instability suggests a very simple explanation. Beyond v_c *all* of the increase in the measured fracture energy is due to the increase in the fracture area caused by microbranch formation. Let us define the relative surface area as the total area per unit crack width created by both the main crack and the microbranches, normalized by that which would be created by a single crack. In Ref. 16 we showed that beyond v_c, this quantity, as a function of the mean crack velocity, increases dramatically. At the highest velocities shown, the contribution to the relative surface area due to the branches dwarfs that of a single crack. Using the measured[16] values of G, we then derived the dependence of the surface area created on the energy release rate. We found that after an initial jump (at approximately v_c), the surface area created is a *linear* function of G whose inverse slope (1.0×10^6 erg/cm^2) is equal to twice the fracture energy. Thus, nearly all of the stored elastic energy in the medium simply goes into creating new surface. This value agrees well with the value of $G(1.1\times10^6$ erg/cm^2) immediately preceding v_c. Mechanisms such as plastic deformation may indeed play a role in determining the basic cost in energy needed to form a unit surface, but the *enhanced* dissipation observed as crack velocities increase beyond v_c is of *dynamic* origin. This dissipation is the direct result of combining a fixed amount of energy expended per unit surface with the large increase in fracture surface production caused by the branching instability. The constant energy cost for surface creation beyond the instability onset indicates that the system ''chooses'' not to dissipate the excess energy stored in the system by increasing the crack velocity, but to divert this energy into the creation of additional surface area. As this excess energy is increased, a higher-energy flux results which leads to longer branches. As the energy flux to the crack is increased still further, we observe the creation of a second generation of microbranches that occur as the first-generation branches bifurcate. This process conceivably occurs as the initial branch reaches v_c, if we assume that a branch follows the same dynamics as the original crack. In this way, the dynamic behavior of a single crack gives rise to a well-defined mechanism for the creation of an eventually fractal surface. The number of generations of branches that are realized in a given experiment is, in this picture, set by the energy density initially stored in the plate.

The jump in the relative surface area observed in Ref. 16 occurs immediately after the instability onset ($G\sim1\times10^6$ erg/cm^2). This sharp initial increase in the slope of the relative surface area as a function of G indicates that when microbranches are very short, the energy cost to create a unit surface is much less than the fracture energy both immediately preceding the instability and in the region where the relative surface area is linearly dependent on G. The reason for this may be due to the nature of the fracture energy in PMMA. The vast majority of the energy needed to create a fracture surface in this material goes into material deformation which occurs in the near vicinity (process zone) of the crack tip. When two cracks (the main crack and microbranch) are sufficiently close to one another (within the same process zone), the total energy needed to deform the surrounding material for the two cracks is nearly the same as for a single crack, and the energy cost to create a unit fracture surface, hence the value of the energy release rate, decreases significantly. Upon leaving the process zone, the fracture energy of a microbranch should be the same as that of the main crack and the jump in the amount of energy needed to form a new surface occurs. This phenomenon may also be a factor in determining the finite minimal branch size (which is approximately the same size as the process zone). The above argument may also provide an explanation for the ''brittle'' or cleavagelike appearance of the patterns formed on the fracture surface (see, e.g., Fig. 14). As long as the microcracks are within the process zone and they do not produce significant additional deformation of the surrounding material, the appearance of the fracture surface that is formed should show few effects of plasticity.

D. The transition from 3D- to 2D-type behavior

A question commonly raised in experiments on thin plates is whether the medium can be considered as two dimensional. By studying the microbranching instability, we can shed some light on this question. The distribution of microbranches throughout the thickness of the plate (the Z direction) is not uniform. In steady-state propagation, more surface area is created by branches in the XY planes adjacent to the plate's exterior, than at its center. The decay in the amount of surface area created by the microbranches appears to be a roughly exponential function of the distance from each exterior surface of the plate. This nonuniform distribution may be due to an inhomogeneous stress as a function of z resulting from the fact that external stress is only directly applied to the medium via the steel bars glued to the plate's outer surfaces (see Sec. II). With these boundary conditions, the energy density may be higher on the plate's exterior surfaces than in its center plane, and we would expect a difference in the amount of surface area created by the branches as a function of z. A typical profile of the surface area created as a function of z is presented in Fig. 16 for a crack propagating at a steady-state velocity of 410 m/s. At crack velocities near v_c the difference in the production of surface area between the plate faces and center is quite pronounced. As the mean velocity increases, however, this difference progressively lessens. Presented in Fig. 17 is the difference in the surface areas created on the plate's face and center, normalized by their average value. This normalized difference decreases monotonically as the velocity increases and

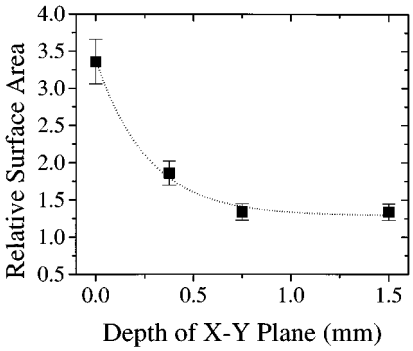

FIG. 16. The relative surface area (defined as the total area per unit width created by both the main crack and microbranches normalized by that which would be crated by a single crack) created solely by microbranches as a function of the depth of the measuring plane (in the Z direction). The data presented were obtained from a crack moving at a steady-state velocity of 410 m/s in a 3-mm-thick plate. Each data point is the average of over 200 branches. The surface production is maximal on the plate's surface ($z=0$), decaying exponentially towards the center of the plate. The dotted line is an exponential fit to the data.

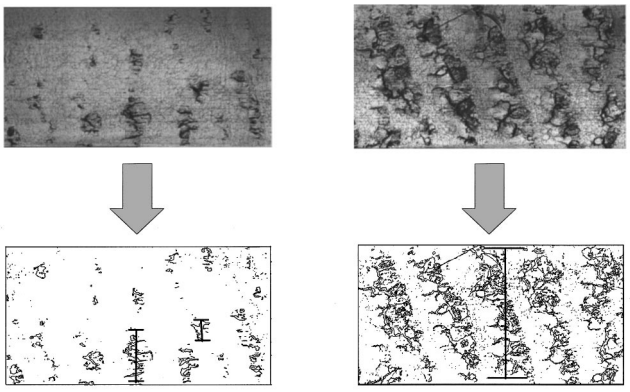

FIG. 18. A photograph of a typical fracture surface (top) and the same pictures after image processing (bottom). The clear difference between the morphology of the ''cleavage zones'' and the rest of the surface, provides a simple way of measuring their width, as demonstrated on the processed pictures. The random spread of the ''cleaved islands'' apparent at $v\sim v_c$ (left) turns into a periodic pattern at higher velocities (right), as the width of the ''cleavage zones'' increases to of the order of the plate's thickness.

reaches a value close to 0 at 550 m/s. We view this velocity as a *transition* velocity at which point the plate becomes effectively 2D.

Is there evidence of this transition to a 2D state on the structure observed on the fractures surface? To see this transition we measure the width of the patterns, defined by the appearance of ''cleavage'' zones (as shown in Fig. 14), on the fracture surface as a function of the mean velocity of the crack. After some image processing, as in the example shown in Fig. 18, the pattern width could be unambiguously identified by utilizing the difference in the textures of the patterns and the zones between them. For velocities only slightly above v_c, as in the case of the distribution of the surface area formation as a function of the sample width, the patterns are far from uniform across the sample with their average width, much smaller than that of the sample. At these relatively low velocities, small ''brittle islands'' are distributed across the fracture surface, as can be seen in Fig. 4(b). The results of the measurement of the mean pattern width as a function of the mean crack velocity are presented in Fig. 19. A sharp transition to a 2D state occurs again at $v=550$ m/s, where the width of the ''cleaved'' zones becomes on the order of the plate's width.[32] As demonstrated in Fig. 4(b), the ''cleaved'' zones at high velocities create clear patterns that extend across the entire width of the plate.

We interpret the pattern width as a measure of the correlation width (in the Z direction) of the microbranches. In this picture, we see the correlation width as continuously increasing above v_c with a possible divergence above 550 m/s. When this correlation length becomes equal to the width of the plate, all the system's characteristics, such as microbranch distribution and the crack-front velocity, become independent of the Z coordinate and the system can be treated as effectively two dimensional. If this assumption is correct, we might expect to find a sharp rise in the correlation between the velocity fluctuations on both sides of the plate, at 550 m/s. An additional prediction of this picture is that the

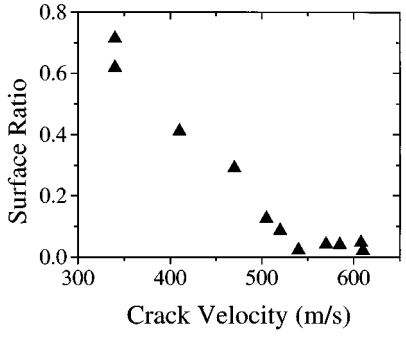

FIG. 17. The surface ratio of a running crack as a function of its velocity. The surface ratio is defined as $(S_{\text{out}}-S_{\text{in}})/(S_{\text{out}}+S_{\text{in}})$where S_{out} and S_{in} are the surface areas created by microbranches on the outer ($z=0$) and center ($z=1.5$ mm) XY planes of the 3-mm-thick plate, respectively. At velocities above 550 m/s $S_{\text{in}}\cong S_{\text{out}}$indicating a homogeneity of microcrack production across the plate's thickness.

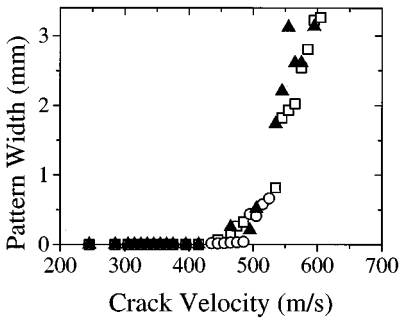

FIG. 19. The width of the ''cleavage zones'' on the fracture surface of a plate (see Fig. 16) as a function of the propagation velocity of the crack. The data plotted were obtained from both 0.8 (circle) and 3-mm (square and triangle) thick plates. At 550 m/s the ''cleavage zone'' (or pattern) width is of the order of the plate's thickness, indicating a 2D state.

divergence of the microbranch correlation width signals the transition from *microscopic* to *macroscopic* crack branching. Since macroscopic branches, unlike microbranches, are 2D phenomena, the transition to a 2D state, is, at the very least, a necessary condition for their formation. If the condition that the branch correlation width surpass the sample width is also sufficient for macroscopic crack branching, we should also find the macrobranching threshold (either as a function of crack velocity or, equivalently, the energy release rate, G) to be dependent on the sample width.

IV. CONCLUSIONS

The experiments described in this paper indicated that the process of dynamic fracture may well be governed by a dynamic instability which describes the transition from a single crack to a multicrack state. In PMMA, the instability leads to the appearance of microbranches accompanying the main crack above a critical velocity of $v_c = 340$ m/s. Above this velocity, as microbranches bifurcate from the main crack, a periodic structure is formed on the fracture surface, and oscillations in the crack velocity are observed. The value of v_c is independent of sample geometry, the external loading of the sample, or the surrounding atmosphere. Beyond the instability onset, all of the characteristic features of the instability scale with the mean velocity of the crack, i.e., the amplitude of the velocity oscillations, the length and distribution of the branches, the mean spacing between branches together with the ''wavelength'' and amplitude of the periodic patterns on the fracture's surface are all linearly dependent on the mean velocity of the crack. This linear dependence leads to a typical time scale, on the order of 1 μs, which we interpret as the branch lifetime. We suggest that many of the following long-standing problems in dynamic fracture are related to the single question of the existence and subsequent evolution of the microbranching instability.

(1) Addressing the question of a *crack-branching criterion*, we demonstrated that microcrack branching occurs at the well-defined velocity, v_c. These microbranches then evolve with increasing velocity into macroscopic branches. We now must ask the question of at what point do microbranches develop into macrobranches.

(2) The mean profile of a branch has a power-law form, independent of the length of the branch or the mean velocity of the crack. Thus, the *branching angle* of a crack becomes a function of the scale of the measurement; at scales on the order of 0.1–0.3 mm the ''branching angle'' is 10°–15° as commonly reported in the literature, but at a resolution of 5 μm, the measured branching angle is about 30°. If the power-law profile of a microbranch holds to smaller scales, we may expect even larger ''branching angles'' to be measured.

(3) A sharp rise in the ''correlation width'' in the system occurs at $v = 550$ m/s. At this velocity the plate becomes effectively two dimensional, as indicated from the distribution of the microbranches along the thickness of the plate together with the width of the patterns formed on the fracture surface. This divergence of the branch correlation width may give rise to a new (sample width dependent) criterion for macroscopic crack branching.

(4) The roughness of fracture surfaces is a direct result of microbranching events. The structure observed on the fracture surface is simply the initial part of the microbranches which then continue to grow within the interior of the sample. Thus, both the surface structure and the increase in the roughness amplitude with the crack velocity are explained.

(5) We find a log-normal distribution of the branch length and the distance between branches. We may then be able to explain the long-observed log-normal distribution in the fragment size of an object which has been fractured at high energy as dynamical in nature and not necessarily, as has long been thought, the result of a cascade of fractures at different scales.

(6) The oscillations in the velocity of the crack result from the repetitive branching process, with a drop in the velocity at the birth of a side branch and acceleration as the branch dies.

(7) Measuring the energy flux into the tip of the crack and comparing it to the total surface area created by the microbranches, shows that the fracture energy is constant and *all* the enhanced dissipation by the crack at velocities above v_c, results from the production of extra surface area by microbranches.

(8) The velocity of a crack does not asymptote to V_R because the crack ''prefers'' to dispose of the energy flowing into it by creating new surface rather than accelerating.

ACKNOWLEDGMENTS

The authors are grateful to M. Marder and S. Gross for numerous enlightening conversations over the course of this work. We acknowledge the United States-Israel binational Science Foundation (Grant No. 92-148) for their support of this work.

[1] L. B. Freund, *Dynamic Fracture Mechanics* (Cambridge University Press, New York, 1990).

[2] K. Ravi-Chandar and W. G. Knauss, Int. J. Fract. **26**, 141 (1984).

[3] See, for example, K. B. Broberg, in *High Velocity Deformation of Solids*, edited by K. Kawata and J. Shioiri (Springer-Verlag, Berlin, 1979), p. 182.

[4] K. Ravi-Chandar and W. G. Knauss, Int. J. Fract. **26**, 65 (1984).

[5] J. G. Michopoulos and P. S. Theocaris, Int. J. Eng. Sci. **29**, 13 (1991).

[6] E. H. Yoffe, Philos. Mag. **42**, 739 (1951).

[7] M. Ramulu and A. S. Kobayashi, Int. J. Fract. **27**, 187 (1985).

[8] H. Gao, J. Mech. Phys. Solids (to be published).

[9] For PMMA see B. Cotterell, App. Mater. Res. **XX**, 227 (1965); in homalite-100 and polycarbonate see Ref. 7; in glass see J. W. Johnson and D. G. Holloway, Philos. Mag. **17**, 899 (1968).

[10] E. S. C. Ching, H. Nakanishi, and J. S. Langer, Phys. Rev. Lett. **76**, 1087 (1996).

[11] J. F. Kalthoff, in *Dynamic Crack Propagation*, edited by G. C.

Sih (Noordhoff, Groningen, 1973), p. 449; P. S. Theocaris and H. Georgiadis, Int. J. Fract **29**, 181 (1985).
[12] S. R. Anthony, J. P. Chubb, and J. Congleton, Philos. Mag. **22**, 1201 (1970).
[13] J. Fineberg, S. P. Gross, M. Marder, and H. L. Swinney, Phys. Rev. Lett. **67**, 457 (1991). Phys. Rev. B **45**, 5146 (1992).
[14] E. Sharon, S. P. Gross, and J. Fineberg, Phys. Rev. Lett. **74**, 5096 (1995).
[15] S. P. Gross, J. Fineberg, W. D. McCormick, M. Marder, and H. L. Swinney, Phys. Rev. Lett. **71**, 3162 (1993).
[16] E. Sharon, S. P. Gross, and J. Fineberg, Phys. Rev. Lett. **76**, 2117 (1996).
[17] M. Marder and X. Liu, Phys. Rev. Lett. **71**, 2417 (1993).
[18] E. Johnson, Int. J. Fract. **55**, 47 (1992); **61**, 183 (1993).
[19] X. P. Xu and A. Needleman, J. Mech. Phys. Solids **42**, 1397 (1994).
[20] L. G. Parletun, Eng. Fract. Mech. **11**, 343 (1979).
[21] M. Isida and H. Noguchi, Int. J. Fract. **54**, 293 (1992)
[22] F. F. Abraham, D. Brodbeck, R. A. Rafey, and W. E. Rudge, Phys. Rev. Lett. **73**, 272 (1994).
[23] The PMMA used has the following static properties: Poisson ratio $=0.35$; $V_R=926$ m/s.
[24] B. Epstein, J. Frank. Inst. **244**, 471 (1947).
[25] A. N. Kolmogoroff, C. R. (Dokl.) Acad. Sci. URSS **31**(2), 99 (1941).
[26] Similar arguments for fluctuations of the crack's velocity can be found in L. B. Freund, J. Mech. Phys. Solids **20**, 141 (1972); J. D. Eshelby *ibid.* **17**, 177 (1969).
[27] See, for example, K.J. Maloy, A. Hansen, E. L. Hinrichsen, and S. Roux, Phys. Rev. Lett. **68**, 213 (1992).
[28] T. Enjoy, K. J. Maloy, A. Hansen, and S. Roux, Phys. Rev. Lett. **73**, 834 (1994); J. Kertesz, V. Horvath, and F. Weber, Fractals **1**, 67 (1993); A. Hansen, E. L. Hinrichsen and S. Roux, Phys. Rev. Lett. **66**, 2476 (1991).
[29] This sharp rise in G as a function of v, derived using the method of caustics in PMMA, was previously observed in optical measurements by A. K. Pratt and P. L. Green, Eng. Fract. Mech. **6**, 71 (1974).
[30] W. Doll, Polymer Eng. Sci. **24**, 798 (1984).
[31] R. P. Kusy and M. J. Katz, Polymer **19**, 1345 (1978).
[32] This transition may be related to the transition in surface roughness in PMMA recently observed by J. F. Boudet, S. Ciliberto, and V. Steinberg, J. Phys. (France) (to be published).